https://doi.org/10.24867/GRID-2022-p74 Original scientific paper

STATISTICAL APPROACH IN FOLD CRACK DISTRIBUTION ANALYSIS

Magdolna Pál , Sandra Dedijer , Ivana Jurič , Gordana Bošnjaković ,
Nemanja Kašiković , Živko Pavlović
University of Novi Sad, Faculty of Technical Sciences, Department of Graphic Engineering and Design, Novi Sad, Serbia

Abstract: *The folding process is one of the most commonly used print finishing operations in graphical production. Therefore, surface damages on coated papers and paperboards, which are frequently appearing during this process, can have significant negative economic and environmental impacts. To reduce the adverse effects, fold crack resistance has become an active field of research. In the last decades, there were several computer-aided visual assessment methods introduced for fold-crack evaluation. These techniques were based on similar concepts of digital image analysis to quantitatively characterise the surface damage, but they had differences in utilisation as well as in the used image feature. In this study, fold crack distribution has been introduced as a new digital image feature for quality assessment. Fold crack distribution can be determined as a measure of crack scattering over the folding line. In this paper descriptive statistics, mean value, standard deviation and coefficient of variance have been used for qualitative characterisation of surface damage. The obtained results for mean value demonstrated increasing tendency by increasing the basis weight and had slightly lower value for samples in machine than cross direction. These results confirm the basic assumptions that on thicker substrates (i.e. on samples with higher basis weight) the cracks are larger, longer or grouped and that the folding process generates higher surface destruction is cross than machine direction. In the case of standard deviation, results suggest that in a case of varying mean values, crack distribution should be defined via coefficient of variation. Based on this analysis, the proposed approach to the calculation of crack distribution can serve as a new image characteristic for the qualitative measurement of the fold-crack resistance of coated papers.*

Key words: fold-crack resistance, damage distribution, coated paper, quality control

1. INTRODUCTION

Surface damages on coated papers and paperboards occurred during the folding process are one of the most frequently encountered problems in the printing industry. Since the folding process is one of the most commonly used operations in the graphical post production it could cause severe financial losses and significant environmentaly adverse effects (Holik, 2013; Soltani et al., 2016; FOGRA, 2020). To reduce the negative effects of folding process, the fold cracking resistance was gaining importance and has become an active field of research. Along with the commonly used mechanical testing methods, different computer-aided assessments have been introduced lately as new techniques for quantitative surface damage characterisation (Barbier et al., 2002; Rättö & Hornatowska, 2010; Yang & Xie, 2011; Barbier et al., 2012; Rättö et al., 2012; Sim et al., 2012; Oh et al., 2015; Oh et al., 2016; Pál et al., 2017; Rajabi Abhari et al., 2018; Najafi et al., 2019; Wang & Ding, 2020; Pál et al., 2021). These newly proposed methods are based on image processing and analysis and have similar basic concept of damage registration, digitization, and image feature calculus. However, they differ in sample preparation method, digitization process, and image processing steps. Furthermore, they have defined only one image feature, only for quantitative damage characterisation, instead of taking advantage of using additional features provided by the computer-aided assessment methods. To overcome these differences in applications and to introduce new digital image features for fold-crack evaluation, detailed research has been conducted.

In this study, a new digital image feature, the fold crack distribution, has been introduced, analyzed and discussed its potential usage for fold-crack quality assessment. The fold crack distribution (in some literature the term distribution is also referred as dispersion) is intended to numerically determine the crack scattering over the folding line. For that purpose, descriptive statistics, mean values with standard deviations and coefficients of variation have been used.

2. METHODS

2.1 Sample preparation

For the purpose of this experiment, glossy coated offset papers have been used in five different nominal basis weights: 90 g/m^2, 115 g/m^2, 130 g/m^2, 150 g/m^2 and 170 g/m^2 (Symbol Freelife Gloss, Fedrigoni, Italy). The increasing basis weight of the selected papers was intended to simulate the expanding tendency of surface damages. The selected papers were determined by basis weight, thickness, ash content, roughness and tensile strength according to the corresponding ISO and TAPPI standards (ISO 536:2012, ISO 534:2005, TAPPI 211om-02, ISO 8791-2:2013, ISO 1924-2:2008) and the results are presented in Table 1.

Table 1: Basic parameters of the selected papers

Properties		Samples				
Nominal values of basis weight [g/m^2]		90	115	130	150	170
Basis weight [g/m^2]		89.72	111.42	125.2	141.65	159.76
Thickness [µm]		65.50	80.20	92.50	113	122.5
Roughness [ml/min]		33.77	14.85	9.55	14.15	10.15
Ash content [%]		40.70	40.23	45.63	40.15	40.26
Tensile strength [kN/m]	MD	4.22	4.62	4.76	6.05	7.16
	CD	2.82	3.01	3.58	4.24	4.91
Elongation [%]	MD	4.67	4.50	4.40	4.85	5.47
	CD	10.37	8.96	10.29	10.55	9.87

Prior to folding, the sample papers were printed on KBA Rapida 75 offset machine in full tone cyan (World Series Cyan, Sun Chemical) to make the cracked surface properly visible. The folding process was done on Horizon AFC546AKT industrial folding machine, using one buckle folding unit with standard folding rollers and roller gap adjustments. The folding process was performed at standard climate conditions (23°C, RH 55%), 48 hours after the printing process. 50 samples of each paper grade were folded in both paper grain directions, marked further on as MD (machine direction) folded and CD (cross direction) folded samples.

2.2 Digital sample acquisition

For the complete investigation, three different digitization devices were used to create digital samples of the folding line. However, for this analysis, only scanned samples were used. The scanning process was done on Canon CanoScan 5600F flatbed scanner with the following setup: scanning resolutions of 1200spi, sRGB color space, no advanced image settings, file type BMP and color depth of 24bit. The scanning window was 4x25mm, and it was set up along the folding line, capturing the damaged areas approximately in the middle of the scanning window. During the scanning process, the paper samples were mounted on a holder with five different inner angles (15°, 30°, 45°, 60°, 90°), placed in a flat position (i.e. 180°) or were completely folded and stacked on each other (for inner angle of 0°). 20 images were generated for each parameter combination (paper grade, fiber orientation and inner angle) and used for image analysis.

2.3 Image analysis and feature extraction

White areas on the images of the coated paper samples are correlated to the surface damages that occurred during the folding process (Rättö & Hornatowska, 2010; Yang & Xie, 2011; Barbier et al., 2012; Rättö et al., 2012; Sim et al., 2012; Oh et al., 2015; Oh et al., 2016; Pál et al., 2017; Rajabi Abhari et al., 2018; Najafi et al., 2019b; Wang & Ding, 2020; Pál et al., 2021). To determine the white pixels` percentage on the digitized folded paper samples and the corresponding additional image features, an image processing algorithm has been developed with the following requirements (Sinha, 2000; Apro et al., 2011; Malek, 2012; Takemetoyo et al., 2007; Nashat et al., 2014; Goncalves et al., 2015; Sengupta et al., 2015): autonomous work, noise suppression, accurate surface damage mapping to the binary image, computationally as simple as a possible solution. The algorithm`s workflow is described below. After the digitization of material samples greyscale images were generated from the original RGB images via red channel extraction. The binary (black and white) images were formed from greyscale ones by segmentation using Otsu automatic thresholding technique. Due to the nature of printed surfaces, additional white pixels were detected alongside the folding line. Since they were not associated with the crack lines but to the large-scale print non-uniformity, detached coating particles, etc., they were eliminated by following masking technique. After the folding line detection with its exact position and direction determined by Hough transform, the image was divided into ten zones and weighted average of white pixel amount was calculated in each zone. Based on the weighted average value, the masking kernel`s width was determined and all the white pixels outside of the masking zone were erased. The resulting binary image in vertical orientation was used as the input file for image feature extraction.

The crack distribution calculus is based on the arithmetic mean value and its corresponding standard deviation of white pixels` sums registered in every row of the analyzed image, according to Equation 1. and 2., respectively:

$$\bar{x} = \frac{1}{n}\left(\sum_{i=1}^{n} x_i\right) \tag{1}$$

$$S = \sqrt{\frac{1}{n-1}\sum_{i=1}^{n}\left(x_i - \bar{x}\right)^2} \tag{2}$$

where: x is a sum of white pixel in one row of the image (later in the text: white pixel count),

n is the number of rows in the image,

$\bar{x}$ is the arithmetic mean value of white pixel count and

S is the standard deviation of white pixel count.

Lower values of standard deviation indicate that the surface damage is evenly distributed along the folding line, while higher values are corresponding to a few and/or bigger and disjoint damages. Although crack distribution is determined via standard deviation, the coefficient of variation is a more interpretable form. Therefore, results are presented in that manner. This image feature can only be applied to samples scanned with inner angle of 15°-180°, where only one folding line was displayed. For samples scanned with inner angle of 0° this approach cannot be used, since 15-20 material samples were visible at the same time, covering the entire observed image and the sum of white pixels in every row represents already an averaged value of those 15-20 folding lines. All the pre-processing, processing and feature extraction steps were done in MATLAB® R2011a package with the corresponding Image Processing Toolbox™.

3. RESULTS

The mean values of average white pixel count, its standard deviation and coefficient of variation were calculated for each paper grade, folding directions and sample placement positions. The obtained results are presented graphically in Figure 1a-b. Similarly, the mean values of white pixels count's standard deviation and coefficient of variation were also calculated along with the relevant descriptive statistics and the results are presented in Figure 2a-b and 3a-b, respectively. Error bars indicate the corresponding standard deviations.

As it can be seen on Figure 1, the white pixel count values have an increasing tendency by increasing the sample papers' basis weight and have slightly higher values for CD folded samples (Figure 1b) than for MD folded ones (Figure 1b), although some deviations can be observed. These results follow the literature data (Barbier et al., 2012; Sim et al., 2012; Oh et al., 2015; Oh et al., 2016; Pál et al., 2017; Wang & Ding, 2020) and the primary hypothesis that papers with higher basis weight and thickness generate larger surface stresses during the folding process**,** especially in the cross direction (CD folding), which causes larger or/and connected surface cracks in the coating layer. The range of obtained values for MD folded samples was 0.66 ÷ 5.58 and for the CD folded samples 0.99 ÷ 9.71. The step-like increment of white pixel count values for CD folded samples was more uniform than for MD folded samples, indicating that the samples` basis weight has a more significant influence on the visible white pixels amount in CD folding than in MD. That difference is more emphasized for lower basis weights (90 g\m^2, 115 g\m^2 and 130 g\m^2) and for sample placement positions from 15° to 90°. For the inner angle of 180°, results were noticeably less uniform, most likely due to the flat scanning position. According to the sample placement positions, the obtained results showed similar changes in both folding directions. For the inner angle of 180°, results were noticeably lower compared to the other sample placement angles. These differences can be attributed to the flat position of the samples during the capturing process. By increasing the inner angle of the sample placement position (from 15° to 90°), the folded samples were slowly opened, while the crack lines gradually closed. Therefore, the surface cracks were reduced in size or disconnected. With the inner angle of 180°, the samples were in flat position, so the cracks were not visible enough (sometimes completely vanished) and the white pixel count values became significantly lower than for the other placement positions.

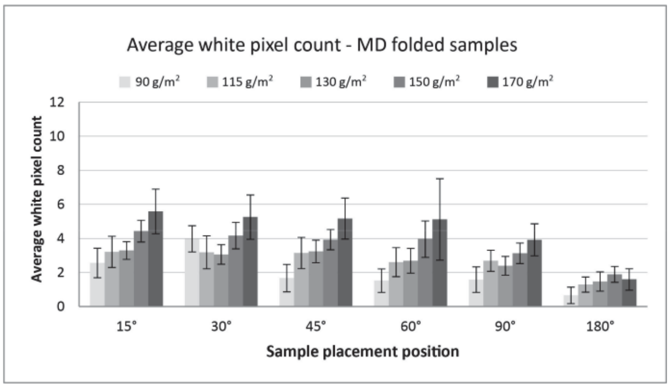

a)

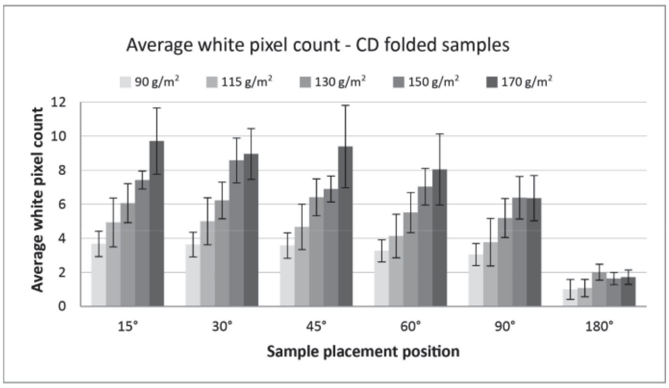

b)

Figure 1: Average white pixel count for machine (a) and cross folded samples (b)

Results for the standard deviation of white pixel count (Figure 2) show some similarities with the mean values regarding the folding directions and the 180° placement position behavior. They have slightly higher values for CD folded samples (Figure 2b) than for MD folded (Figure 2a) and samples with inner angle of 180° gave visibly lower results, especially in CD folding direction. Besides similarities, there are two differences among the obtained results. One is regarding to the samples basis weight, another to the sample placement positions from 15° to 90°. Namely, there is no consistent step-like increment with the samples' basis weight (especially in MD folding direction) and the values for different placement positions were similar to each other. The range of obtained values were 2.04 ÷ 3.48 for MD folded samples and 2.50 ÷ 4.51 for CD folded ones, while for the inner angle of 180° the ranges were 1.22 ÷ 2.10 for MD samples and 1.44 ÷ 2.15 for CD samples. These results suggest that all samples had more or less similar crack dispersion over the folding line. However, after a detailed visual analysis of the original sample images, it has been proven not to be the case. Papers with lower basis weight have a few, minor or moderate crack patches along with fine crack lines randomly scattered over the folding line. On the other hand, on papers with higher basis weight, more intense surface cracks were registered with an even distribution of longer, thicker and connected crack lines with occasional larger crack patches. Thus, the results in this form do not reveal much about the nature of the coating damage, primarily due to the differences in the mean values. Therefore, the basic idea for using standard deviation for crack distribution metric cannot be validated without knowing the mean values. For appropriate data analysis in such a case of varying mean values, the crack distribution metric (at least in this study) should be defined via the coefficient of variation.

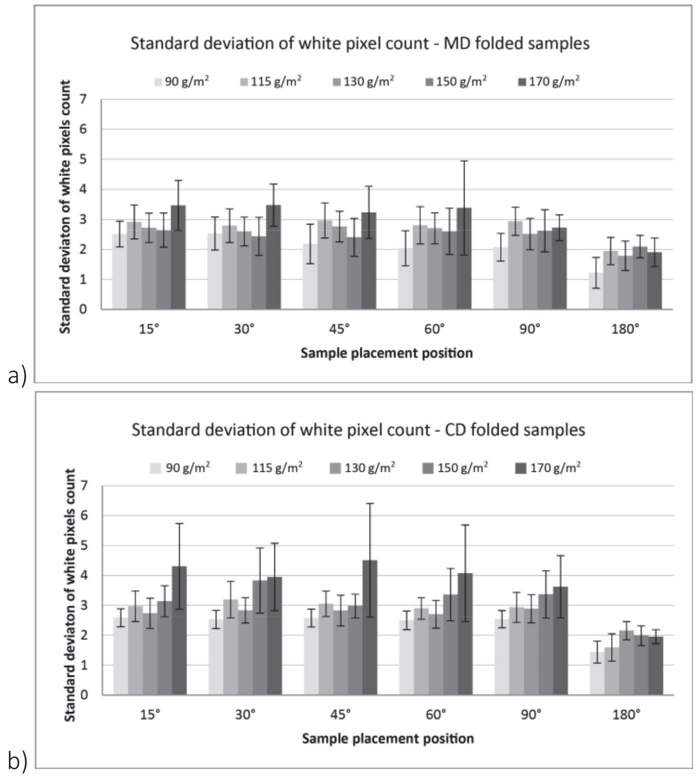

Figure 2: Standard deviation of white pixel count for machine (a) and cross folded samples (b)

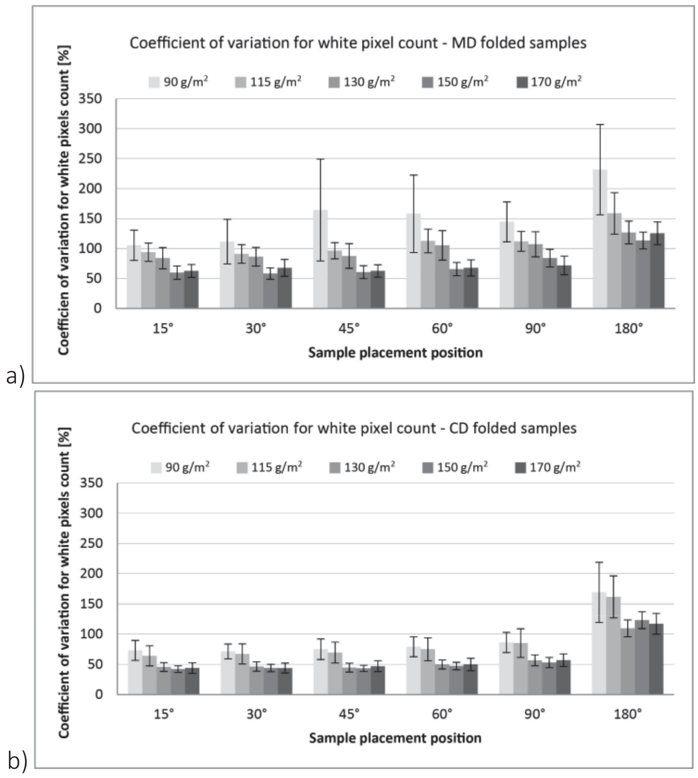

Figure 3: Coefficient of variation for white pixel count of samples folded in machine (a) and cross direction (b)

Results of coefficient of variation for white pixel count [%] (Figure 3a-b), in general, have decreasing tendency by increasing the sample papers' basis weight and have significantly lower values for CD folded samples than for MD folded ones. Although, there are some minor deviations mostly for the thickest paper (170 g\m^2), the results follow gradual stepwise changes as suspected by (Barbier et al. 2012, Sim et al. 2012, Oh et al. 2015, Oh et al. 2016, Pál et al. 2017 Wang and Ding 2020). Papers with higher basis weight and thickness generate larger, longer or/and connected surface cracks in the coating layer which are evenly distributed along the folding line, thus resulting in low values of coefficient of variation. For samples folded in cross direction, this trend is more emphasized and extends to thinner papers. These results indicate that even samples with lower basis weights get long and connected crack lines during CD folding. The more uniform, step-like decreasing of coefficient of variation values for MD folded samples (Figure 3a) indicates that basis weight has a more significant influence on the crack distribution in MD folding than in CD. That trend is more noticeable for lower basis weights (90 g\m^2, 115 g\m^2 and 130 g\m^2) and for the sample placement positions from 15° to 90°. The range of obtained values for the mentioned samples were 84.03% ÷ 164,39% for MD folding, and 44.66% ÷ 86.28% for CD folding. Samples with the two highest basis weight (150 g\m^2 and 170 g\m^2) and the same inner angles had ranges from 58.38% up to 84.09% for MD folding and from 42.17% up to 57.04% for CD folding. The surprisingly similar values for all CD folded samples with inner angles between 15° and 90° suggest that sample placement position has little or no effect on crack distribution.

By comparing the results according to the sample placement, similar changes could be noticed in both folding directions. For the inner angle of 180°, results were noticeably higher than the other sample placement angles (the ranges were 113.58% ÷ 231.78% for MD samples and 109.64 ÷ 169.09 for CD samples). This could refer to the fact that by increasing the inner angle of sample placement, crack lines were gradually closing at the very tip of the folding line, reducing the total area of surface damage. At an angle of 180°, the samples were completely flat, and only large crack spots remained visible, randomly scattered along the fold line, giving rise to typically high values of the coefficient of variation.

4. CONCLUSIONS

In this study, the applicability of crack distribution via descriptive statistics as a new digital image feature for fold-crack assessment has been presented and analyzed.

The obtained results, in general, demonstrated that the mean white pixel count has an increasing tendency by increasing the basis weight of the substrates and had a slightly lower value for samples folded in the machine than cross direction. These results confirm the basic assumptions that on thicker substrates (i.e. on samples with higher basis weight), the crack lines are larger, longer or grouped and that the folding process generates higher surface destruction in cross than machine direction.

The basic concept of using standard deviation for crack distribution measure seems to be correct since lower values indicate evenly distributed surface damages, often in the form of long and thick crack lines over the entire folded area. In comparison, higher standard deviation values correspond to a few, small or medium, but usually disjoint cracks. However, instead of the standard deviation, the coefficient of variation can provide more accurate results for a more realistic characterization of crack scattering, regardless of the difference in mean values. Based on the obtained results, it can be concluded that the proposed approach to the calculation of crack distribution can serve as a new image characteristic for the qualitative measurement of the fold-crack resistance of coated papers.

5. ACKNOWLEDGMENTS

This research (paper) has been supported by the Ministry of Education, Science and Technological Development through project no. 451-03-68/2022-14/ 200156 “Innovative scientific and artistic research from the FTS (activity) domain”.

6. REFERENCES

Apro, M., Pal, Sz. & Dedijer, S. (2011) Evaluation of single and multi-threshold entropy-based algorithms for folded substrate analysis. *Journal of Graphic Engineering and Design*. 2 (2), 1-9.

Barbier, C., Larsson, P. L. & Östlund, S. (2002) Experimental investigation of damage at folding of coated papers. *Nordic Pulp and Paper Research Journal*. 17 (1), 34-38. Available from: doi: 10.3183/npprj-2015-30-02-p361-368

Barbier, C., Rättö, P. & Hornatowska, J. (2012) Coating models for an analysis of cracking behaviour between folded paper and creased board. In: *12th TAPPI Advanced Coating Fundamentals Symposium, 2012, Atlanta GA, USA.* pp. 5-16*.*

FOGRA. (2020) *Laboratory method for the practical and reproducible determination of the residual strength of papers for heatset web offset printing*. Available from: https://fogra.org/en/research/offset-printing/residual-strength-of-heatset-we b-offset-papers-42029 [Accessed 15th June 2022]

Goncalves, N., Carvalho, V., Belsley, M., Vasconcelos, R. M., Soares, F. O. & Machado, J. (2015) Yarn features extraction using image processing and computer vision – A study with cotton and polyester yarns. *Measurement*. 68, 1-15. Available from: doi: 10.1016/j.measurement.2015.02.010

Holik, H. (2013) *Handbook of Paper and Board, Volume 1-2. Second, Revised and Enlarged Edition*. Weinheim, Germany, Wiley-VCH Verlag GmbH & Co. KGaA.

International Organization for Standardization. (2005) ISO 534:2005. *Paper and board, Determination of thickness, density and specific volume*. Geneva, International Organization for Standardization.

International Organization for Standardization. (2008) ISO 1924-2:2008. *Paper and board - Determination of tensile properties - Part 2: Constant rate of elongation method (20 mm/min).* Geneva, International Organization for Standardization.

International Organization for Standardization. (2012) ISO 536:2012. *Paper and board - Determination of grammage.* Geneva, International Organization for Standardization.

International Organization for Standardization. (2013) ISO 8791-2:2013. *Paper and board - Determination of roughness/smoothness (air leak methods) - Part 2: Bendtsen method.* Geneva, International Organization for Standardization.

Malek, A. S. (2012) *Online fabric inspection by image processing technology*. PhD thesis. University of Upper Alsace.

Najafi, S. M. H., Bousfeld, D. W. & Tajvidi, M. (2019) Cracking at the fold in double layer coated paper: the influence of latex and starch composition. *Tappi Journal*. 18 (2), 93-99. Available from: doi: https://doi.org/10.32964/TJ18.2.93

Nashat, S., Abdullah, A. & Abdullah, M. Z. (2014) Machine vision for crack inspection of biscuits featuring pyramid detection scheme. *Journal of Food Engineering*. 120 (1), 233-247. Available from: doi: 10.1016/j.jfoodeng.2013.08.006

Oh, K., Seo, D., Youn, H. J., Lee, Y .M., Yeu, S. U. & Lee, H. L. (2016) Effects of coating composition and folding direction on the fold cracking of coated paper. *Nordic Pulp and Paper Research Journal*. 31 (2), 347–353. Available from: https://doi.org/10.3183/npprj-2016-31-02-p347-353

Oh, K., Sim, K., Jung, Y. B., Youn, H. J., Lee, H. L., Lee, Y. M. & Yeu, S. U. (2015) Effect of coating binder on fold cracking of coated paper. *Nordic Pulp and Paper Research Journal*. 30 (2), 360–367. Available from: https://doi.org/10.3183/npprj-2015-30-02-p361-368

Pál, M., Dedijer, S., Koltai, L., Gregor-Svetec, D., Cigula, T., Pavlović, Ž. & Milić-Keresteš, N. (2021) Fold cracking of coated papers: Investigation on automated computer-aided visual assessment method. *Nordic Pulp and Paper Research Journal*. 36 (4), 626-642. Available from: https://doi.org/10.1515/npprj-2021-0041

Pál, M., Novaković, D., Dedijer, S., Koltai, L., Jurič, I., Vladić, G. & Kašiković, N. (2017) Image processing based quality control of coated paper folding. *Measurement*. 100, 99-109. Available from: 10.1016/j.measurement.2016.12.033

Rajabi Abhari, A., Lee, H. L., Oh, K., Im, W., Lee, J. H., Lee, S. & Kim, S. (2018) Suspension-polymerized latex as an additive for surface sizing and its effect on fold cracking of coated paper. *BioResources.* 13 (4), 7640-7653. Available from: doi:10.15376/biores.13.4.7640-7653

Rättö, P. & Hornatowska, J. (2010) The influence of coating colour composition on the crack area after creasing. *Nordic Pulp and Paper Research Journal*. 25 (4), 488-494. Available from: doi:10.3183/npprj-2010-25-04-p495-501

Rättö, P., Hornatowska, J. & Barbier, C. (2012) Influence of the distribution of the shape and size distribution of pigment particles on cracking in coating layers during creasing. *Nordic Pulp and Paper Research Journal*. 27 (4), 714-720. Available from: doi:10.3183/NPPRJ-2012-27-04-p714-720

Sengupta, A., Roy, A. & Sengupta, S. (2015). Development of low cost yarn parameterisation unit by image processing. *Measurement*. 59, 96-109, Available from: doi:0.1016/j.measurement.2014.09.028

Sim, K., Youn, H. J., Oh, K. D., Hak Lae Lee, H. L., Han, C. S., Yeu, S. U. & Lee, Y. M. (2012) Fold cracking of coated paper: The effect of pulp fiber composition and beating. *Nordic Pulp and Paper Research Journal*. 27 (2), 445-450. Available from: doi:10.3183/npprj-2012-27-02-p445-450

Sinha, S. K. (2000) Automated underground pipe inspection using a unified image processing and artificial intelligence methodology. PhD thesis. University of Waterloo.

Soltani, M., Rohani, A. A., Ramazani, O., Naji, H. R., Hazandz, A. H., Simonot, L. & Bakar, E. S. (2016) UV-curable coating process on CMYK-printed duplex paperboard, Part II: effects of nano-TiO2 modification. *BioResources.* 11 (1), 1930-1940. Available from: doi:10.15376/biores.11.1.1930-1940

Takemetoyo, Y., Miyauchi, H., Lacasse, M. A., Enomoto, N., Ito, A. & Tanaka, K. (2007). Quantification of surface crack damage of construction sealants. In: *International Conference on Building Envelope Systems and Technology*, *ICBEST 2007, 28 March 2007, Bath, UK*. National Research Council Canada. pp. 1-10.

TAPPI Standards. (2007) T 211 om-93 *Ash in wood, pulp, paper and paperboard: combustion at 525°C*. Peachtree Corners, Georgia, USA, TAPPI.

Wang, Q. & Ding, N. (2020) Coating factors influencing the fold cracking of coated papers. *Nordic Pulp and Paper Research Journal*. 35 (3), 419-431. Available from: doi:10.1515/npprj-2019-0051

Yang, A. & Xie, Y. (2011) From theory to practice: Improving the foldcrack resistance in industrially produced triple coated paper. In: *Tappi PaperCon Conference*, *1-4 May 2011, Covington, Kentucky, USA*. pp. 1845-1858.